17.2 SODAR BASED WIND PROFILES AS MODEL INPUTS: UNDERSTANDING THE ROLE OF ATMOSPHERIC CONDITIONS IN ASSESSING THE QUALITY OF THE DATA

Gennaro H. Crescenti
Air Resources Laboratory Field Research Division
National Oceanic and Atmospheric Administration
Idaho Falls, Idaho

Robert A. Baxter
Parsons Engineering Science
Pasadena, California

1. INTRODUCTION

With the increased employment of sophisticated transport and dispersion models that require wind profiles, a greater emphasis has been placed on reliably acquiring these data. The recent release of updated guidance by the U. S. Environmental Protection Agency (U. S. EPA 1987, revised 1999) on the quality assurance (QA) and quality control (QC) for Doppler sodars will lead to greater acceptance of this technology in regulatory-driven monitoring programs. As with any instrument used in a monitoring program, the independent audit process is essential for assessing the proper operation and performance of that particular sensor. For example, tethersondes, kites, or nearby towers are often used in the assessment of a sodar. However, while the methodology and statistical techniques used for comparison purposes are well established, the expected scatter between wind measurements acquired by a sodar and audit instrument can vary widely as a function of atmospheric conditions and stability. In many instances, fault is often assigned to the sodar when large scatter is observed between measurement systems.

Data acquired during a ground-based remote sensor characterization study at the Boulder Atmospheric Observatory (BAO) clearly demonstrates that large differences between tower and sodar winds exist during nonhomogeneous conditions. The results of this study will be useful for understanding statistical differences encountered during the audit process. It should be noted that this is not a comparison study of one sodar against another.

2. DATA

The study was conducted at the BAO over a three-week period in April 1995. R. M. Young wind monitors were mounted at 10, 50, 100, 200, and 300 m on the BAO tower to measure scalar and vector wind speed, vector wind direction, and standard deviation of the unit vector wind direction (σ_θ). These anemometers were mounted approximately 2 m from the tower on booms oriented towards the south-southeast (154°). Vaisala HMP-35 probes were placed in fan-aspirated radiation shields at the same levels to measure air temperature and relative humidity. The intakes of the radiation shields were at least 0.5 m away from the tower to minimize the effect of solar heating. Two platinum resistance temperature probes were also placed inside fan-aspirated radiation shields at 10 and 50 m to measure temperature difference (ΔT). Solar radiation was measured with an Eppley Laboratory Precision Spectral Pyranometer. These sensors were sampled at 1 Hz and recorded as 15-min averages.

Commercial manufacturers of Doppler sodars (in alphabetical order: AeroVironment, Metek, Radian, and Remtech) were invited to participate in the study. Three companies (AeroVironment, Metek, and Radian) accepted the invitation. A total of four Doppler sodars were deployed around the perimeter of the BAO tower (~ 275 m) by engineers and/or technicians of their respective companies. The oblique angle beams of the sodars were oriented away from the tower so that reflections from the tower and its guy wires were avoided. In addition, this strategy minimized any potential contamination of acoustic pulses from one sodar system to another. All four sodars recorded wind velocity profiles as 15-min averages. Sodar specifications are listed in Table 1.

3. PERFORMANCE AUDITS

Prior to the start of the study, performance audits were conducted on the sodars in accordance with the most current guidance available from the U. S. EPA (1987, 1995). The audits provided an independent assessment that the sodars were setup and operating in accordance with the manufacturers recommendations (Baxter 1996).

3.1 *Equipment Alignment*

The orientation of an antenna with respect to azimuth directly affects the accuracy of the sodar-derived wind direction while the level of an antenna with respect to horizontal directly affects the calculation of the component wind velocities. Where applicable, a tripod-mounted Brunton Pocket Transit was used to verify the orientation and level of the sodar antennas. Local magnetic deviation was corrected by solar siting (U. S. EPA 1995). The audit found that all of these antennas were aligned to within 1° in azimuth. Antenna levels were checked using the inclinometer integral to the transit. All four sodars were found to be with ±0.5° from horizontal. EPA criteria for acceptable uncertainty in azimuth and level are ±2° and ±0.5°, respectively.

Corresponding author address: Gennaro H. Crescenti, Air Resources Lab. Field Research Division, 1750 Foote Dr., Idaho Falls, ID 83402; e-mail: jerry.crescenti@noaa.gov

Table 1. Doppler sodar specifications.

	AeroVironment 4000	Metek MODOS	Radian 600	Radian 600PA
Type	phased-array	3-axis	3-axis	phased-array
Frequency (Hz)	4500	2009	1850	2125
Pulse Width (ms)	50	150	150	150
Pulse Interval (s)	1	4	4	4
Zenith Angle (°)	18	20	18	14.87
U-Axis Beam Direction (°)	173	101	302	349
V-Axis Beam Direction (°)	83	11	215	259
Minimum Height (m)	10	50	50	50
Maximum Height (m)	200	650	700	700
Gate Width (m)	5	25	25	25

3.2 *Evaluation of Site Characteristics*

Evaluation of site characteristics included identification of active and passive noise sources. Active noise included artificial and natural sources at and near the BAO and included traffic from Interstate-25, equipment trailer air conditioners, and birds. In addition, two active noise sources were common to all of the sodars. The first was a radio acoustic sounding system (RASS) that operated at the BAO. The RASS acoustic sources were active two times per hour for 5 min. The operating frequency of the RASS was outside the operating range of all sodars except the MODOS. Metek took precautions against interference by orienting their oblique angle antennas away from the RASS. The second active noise source was wind-generated due to the tower and its guy wires. During windy conditions (> 10 m s^{-1}), a "whistling" effect was created. The frequency of the noise varied with changing wind speeds. However, audit capabilities at the time were unable to identify specific frequencies of wind-generated noise. Since then, Crescenti and Baxter (1998) have been able to identify the frequencies of various noise sources using spectral analysis programs. Acoustic noise levels were measured at the BAO using a Realistic 33-2055 digital sound level meter. The maximum level was approximately 64 dB with average noise levels < 50 dB.

Ideally, a site should be relatively clear of obstacles that could act as potential fixed-echo reflectors (passive noise) for sodars. Obstacle vista tables were constructed for the identification of all natural and man-made objects surrounding each sodar. These tables included information on an objects azimuth, elevation angle, and distance from a sodar. The results of the site evaluations identified the locations of each sodar as generally acceptable (Baxter, 1996). There were a number of reflective sources that could potentially contaminate the data, but each manufacturer oriented the oblique angle antenna beams away from those objects. In particular, the most significant reflective source was the BAO tower and its guy wires. Minor sources included a variety of small buildings used for electronics and data acquisition systems.

Another sodar system check was a so-called "listen only" test (sodar transmitters are turned off but the receivers remain on). This test can help determine if any background noise level produces a "measured" wind velocity. In practice, no valid wind values should be reported by a sodar. However, if any "valid" values are reported, then there may be an active noise source-generating frequencies in the operating range of the sodar. All sodars tested during the audit displayed only invalid data during this test.

3.3 *Simulated Wind Test*

A simple wind profile simulation was applied to each sodar using a device developed by Baxter (1995) known as the Acoustic Pulse Transponder (APT). This system first detects the transmitted acoustic pulse from a sodar antenna then transmits a preprogrammed pulse sequence back at the sodar. The pulse sequence consists of one or more sequential frequencies at specifically timed intervals that represent known frequency offsets from the sodar. The frequency offsets and time of the pulses simulate a wind profile along each of the sodar component axes. The APT has an accuracy of 1 Hz from 1390 to 4606 Hz. The accuracy of the pulse timing is 2 ms, which corresponds to an altitude resolution of better than 1 m.

The APT was programmed to simulate wind velocities of 3 to 4 m s^{-1} in the lower portion of the sodar operating range. The upper portion of the profile was programmed to smoothly increase wind velocities to 7 to 8 m s^{-1} in the opposite direction. The results of the APT tests show agreement for all sodars to within ±0.2 m s^{-1}.

4. METHODOLOGY

Most evaluation studies have used simple statistical techniques to assess the overall reliability of sodar measurements. For example, many investigators use the linear correlation coefficient r. However, when using r to assess the reliability of both wind speed and wind direction from a sodar against tower-based values, two separate values must be determined. Crosby et al. (1993) proposed a definition for a vector correlation coefficient r_v in which the effects of both magnitude and direction are included in a simple scalar value that is a measure of the degree of association between the vectors of interest. By definition, a perfect correlation between two sets of vectors yields a value of $r_v = 2$. Zero correlation exists when $r_v = 0$.

Other statistics of comparison are the bias (systematic error) B, comparability (root-mean-square difference) C, and precision (standard deviation) S (Hoehne 1971). Many investigators often compute these statistics for an entire data set regardless of atmospheric conditions or stability. When the data sets were subdivided, it was often for day versus night so that Doppler sodars could be evaluated for convective (unstable) versus laminar (stable) conditions, respectively. This study extended this methodology by defining various objective measures of atmospheric conditions and stability based on tower data.

Eight different measures of atmospheric conditions and stability were used in this study to measure the statistical characteristics of these sodars. They include the relative humidity (RH), Pasquill-Gifford (PG) stability class, time of day, scalar wind speed (SS), the standard deviation of the unit vector wind direction (σ_θ), wind shear (S_h), Brunt-Vaisala frequency (N_{BV}), and the bulk Richardson number (R_B). These parameters were chosen since they are easily derived from tower-based measurements.

Molecular attenuation of acoustic signals from Doppler sodars significantly increases with decreasing relative humidity, especially for relative humidity less than 40%. Statistical estimates were derived for five classes of surface (10-m) relative humidity. The statistics were generated for relative humidities between 0 - 20%, 20 -40%, 40 - 60%, 60 - 80%, and 80 - 100%.

PG stability was determined using the solar radiation/delta-T method (Coulter 1994). One of six stability classes was determined from 10-m tower wind speed, incoming solar radiation, and ΔT. These stability classes are useful in characterizing an unstable (A, B, C), neutral (D), or stable (E, F) boundary layer.

Time of day was divided into four categories: dawn, day, dusk, and night. The dawn and dusk were included to examine transitional stability regimes. Dawn is defined as the time in the early morning when the Sun is between 10° below the horizon to 20° above the horizon. Dusk is defined as the time in the late afternoon when the Sun is between 10° above the horizon to 20° below the horizon.

Strong winds can generate localized noise that can potentially interfere with Doppler sodar operations. The surface (10-m) scalar wind speed was subdivided into four categories: near calm (< 2 m s^{-1}), light wind (2 - 5 m s^{-1}), moderate wind (5 - 10 m s^{-1}), and strong wind (> 10 m s^{-1}).

Values of 10-m σ_θ were used to measure the horizontal homogeneity of the wind field. Four categories were created: very homogeneous (< 10°), moderately homogeneous (10 - 20°), moderately nonhomogeneous (20 - 30°), and very nonhomogeneous (> 30°).

A simple measure of mechanical mixing can be estimated by computing the wind shear. S_h was determined by the wind velocity difference between 10 and 50 m. Four categories were created: no wind shear (< 0.02 s^{-1}), light wind shear (0.02 - 0.04 s^{-1}), moderate wind shear (0.04 - 0.06 s^{-1}), and strong wind shear (> 0.06 s^{-1}).

A simple measure of the thermal mixing can be estimated by computing the square of the Brunt-Vaisala frequency. For this study, N^2_{BV} was determined by the temperature difference between 10 and 50 m. Four categories were created: unstable (< 0 s^{-2}), slightly stable (0 - 0.001 s^{-2}), moderately stable (0.001 - 0.002 s^{-2}), and strongly stable (> 0.002 s^{-2}).

The bulk Richardson number R_B is the ratio of thermal to mechanical mixing. R_B is computed from temperature and wind at 10 and 50 m. Four categories include strongly unstable (< -0.5), moderately unstable (-0.5 - 0.25), moderately stable (0.25 - 1), and strongly stable (> 1). Equations for S_h, N_{BV}, and R_B are given by Stull (1988).

Some data were eliminated in order to avoid an artificial bias or scatter. Data were not considered when the tower-based vector wind speed was less than 0.5 m s^{-1} (i.e., below the starting threshold of the wind monitor). In addition, data were not considered when the wind direction was between 302° clockwise to 32°. This was done to avoid tower-generated turbulence and is consistent with the methodology used by Kaimal (1986).

5. ANALYSIS

The bias for wind speed and direction for all sodars for all cases and for all levels was between -0.5 to 1.0 m s^{-1} and -5 to 10°, respectively. The scatter (comparability and precision) was quite good. In general, S for sodar wind speed ranged between 0.5 and 1.0 m s^{-1}. Values of S for wind direction ranged between 10 and 30°. Values of r were also quite good for the sodar wind speed and directions with values in excess of 0.90. These statistics are comparable and in some cases, better to those determined by previous comparison studies (Crescenti, 1997). Values of r_v are exceptionally good with values exceeding 1.8 for all measurement levels (Table 2). In general, r_v decreases with height. This is due, in part, to spatial variability between the tower and the measurement volume of the sodar. Recall that the oblique angle beams of each sodar were oriented away from the tower. The distance between the tower and sodar sampling volume increases as $z\tan\alpha$, where z measurement height and α is the oblique angle of the sodar from the zenith.

Crescenti (1999) showed that sodar range was limited under very dry conditions. However, no apparent relationship exists between the statistics as a function of the relative humidity. All sodars show similar values of S for each RH classification. Some values of r_v for very dry conditions (RH < 20%) tend to suggest that there is more disagreement between tower wind and sodar wind vectors.

Significant scatter is observed in the sodar data under very convective conditions (PG class A, B). Values of S range from 0.6 to 0.9 m s^{-1} for speed and 30 to 60° for direction. The amount of scatter significantly decreases with increasing stability. In general, the least amount of scatter is seen for classes E and F. Values of S range from 0.3 to 0.4 m s^{-1} and 5 to 15° for class E and F. Values of r_v are quite good (Table 2) for classes C and D (1.85 to 1.95) and exceptionally high (~ 1.95) under the most stable atmospheric conditions (class E and F).

Similar behavior is reflected in these statistics as a function of time of day. In general, the best agreement between tower and sodar occurs during dawn, dusk and night. Daytime conditions usually show the most variability. Again, this is due to the convective nature of the boundary layer, especially under light wind conditions. While scatter in wind speed and direction is greater for daytime conditions, overall agreement is still quite good.

Table 2. Vector correlation coefficients as a function of PG stability and R_B.

	All Cases	A	B	C	D	E	F	<-0.5	-0.5 - 0.25	0.25 -1	>1
AV 4000											
10 m	1.83	1.55	1.88	1.92	1.87	1.17	0.91	1.75	1.82	1.84	1.75
50 m	1.95	1.59	1.88	1.95	1.97	1.94	1.88	1.89	1.95	1.98	1.97
100 m	1.93	1.37	1.79	1.88	1.95	1.94	1.97	1.83	1.93	1.97	1.95
Metek MODOS											
50 m	1.90	1.13	1.52	1.75	1.95	1.96	1.62	1.69	1.94	1.92	1.89
100 m	1.89	0.82	1.31	1.82	1.95	1.95		1.56	1.93	1.92	1.86
200 m	1.84	0.68	1.13	1.76	1.89	1.93	1.93	1.47	1.93	1.79	1.38
300 m	1.49	0.64	1.01	1.68	1.50	1.58		1.27	1.67	0.93	1.28
Radian 600											
50 m	1.93	1.14	1.70	1.92	1.95	1.84	1.82	1.76	1.95	1.92	1.88
100 m	1.95	0.96	1.67	1.91	1.96	1.94	1.87	1.75	1.96	1.94	1.92
200 m	1.93	0.88	1.55	1.91	1.97	1.96	1.94	1.66	1.96	1.96	1.88
300 m	1.83	0.81	1.51	1.88	1.89	1.96	1.91	1.60	1.95	1.93	1.90
Radian 600PA											
50 m	1.86	0.80	1.65	1.83	1.88	1.57	1.53	1.69	1.83	1.90	1.81
100 m	1.93	1.14	1.58	1.90	1.96	1.94	1.91	1.71	1.95	1.95	1.92
200 m	1.92	0.92	1.64	1.87	1.96	1.93	1.96	1.68	1.95	1.96	1.84
300 m	1.79	1.08	1.65	1.80	1.85	1.77		1.64	1.92	1.88	1.83

Not surprisingly, significant variance is observed for near calm winds. Under such conditions, large variations can be expected in the wind field and substantial disagreement can occur, even over relatively short distances of a few hundred meters. As expected, less scatter is found when the winds are light to moderate. Values of S for wind direction are quite good for moderate wind speeds. Unfortunately, very little data was acquired by the sodars under strong winds (> 10 m s^{-1}). This is due to wind-generated noise that interferes with sodar operation. This has been a recurring theme found by many other investigators (Crescenti 1997).

The most dramatic statistics are seen as a function of σ_θ (Figs. 1 and 2). Values of r and r_v degrade substantially as σ_θ increases to larger values. Conversely, the best agreement is found when σ_θ < 10°. Values of S range from 5 to 10° when σ_θ < 10° and ~ 50° when σ_θ > 30°. Large values of σ_θ are associated with a nonhomogeneous conditions. Spatial separations between tower and sodar can cause significant disagreement.

The statistics are also very dramatic as a function of S_h. Values of S generally improve with larger wind shear for wind speed. However, the improvement is very dramatic for the wind direction comparisons. With little or no wind shear (< 0.02 s^{-1}), S ranges from 30 to 40°. However, for strong wind shear (> 0.06 s^{-1}), S ~ 5°. When the wind speed and wind directions are combined and analyzed as vectors, values of r_v are exceptional (> 1.9) when wind shear exists. Strong wind shear provides stronger scatter given equal background potential temperature gradients (Gaynor 1979). The turbulence continually creates and destroys microscale (0.01 - 10 m) temperature gradients, thereby enhancing acoustic backscatter.

Once again, the variance between tower and sodar measurements is largest for unstable conditions (N^2_{BV} < 0) and smallest during stable conditions (N^2_{BV} > 0). The most dramatic statistics are seen for the wind direction where values of S are ~ 5° for moderately to strongly stable conditions.

The best agreement was also found for the moderately unstable (-0.5 to 0.25) and moderately stable (0.25 - 1) conditions. For strongly stable conditions (R_B > 1), variance increases for both wind speed and wind direction measurements. For strongly unstable conditions (R_B < -0.5), the variance is largest.

6. DISCUSSION

It should be pointed out that this is a limited data set that was collected at a specific location during a specific time of year. A full cross section of possible conditions was not encountered. Nevertheless, a sufficient number of data points were collected to demonstrate the behavior of these sodars under various atmospheric conditions.

Overall, sodar winds compare quite well against tower-based measurements. In general, more variance was observed during convective and light wind conditions. Conversely, the scatter was small for stable conditions.

What are the implications? Audits or other independent wind measurement comparisons conducted in an unstable boundary layer can show considerable disagreement between the sodar and the "ground-truth" measurement platform. This is not to say that the sodars acquire invalid data. Rather, the inhomogeneity of the boundary layer can produce conflicting numbers from sensors separated on the order of several hundred meters. Thus, any comparison between sodar and reference measurement system should be conducted over at least one full day to assure that sodar wind data are valid.

It is also important to point out that the scatter in these statistics also represents errors in the tower-based measurements due to wind flow distortion. Unfortunately, many investigators have attributed the uncertainty strictly to the sodar (Crescenti 1997).

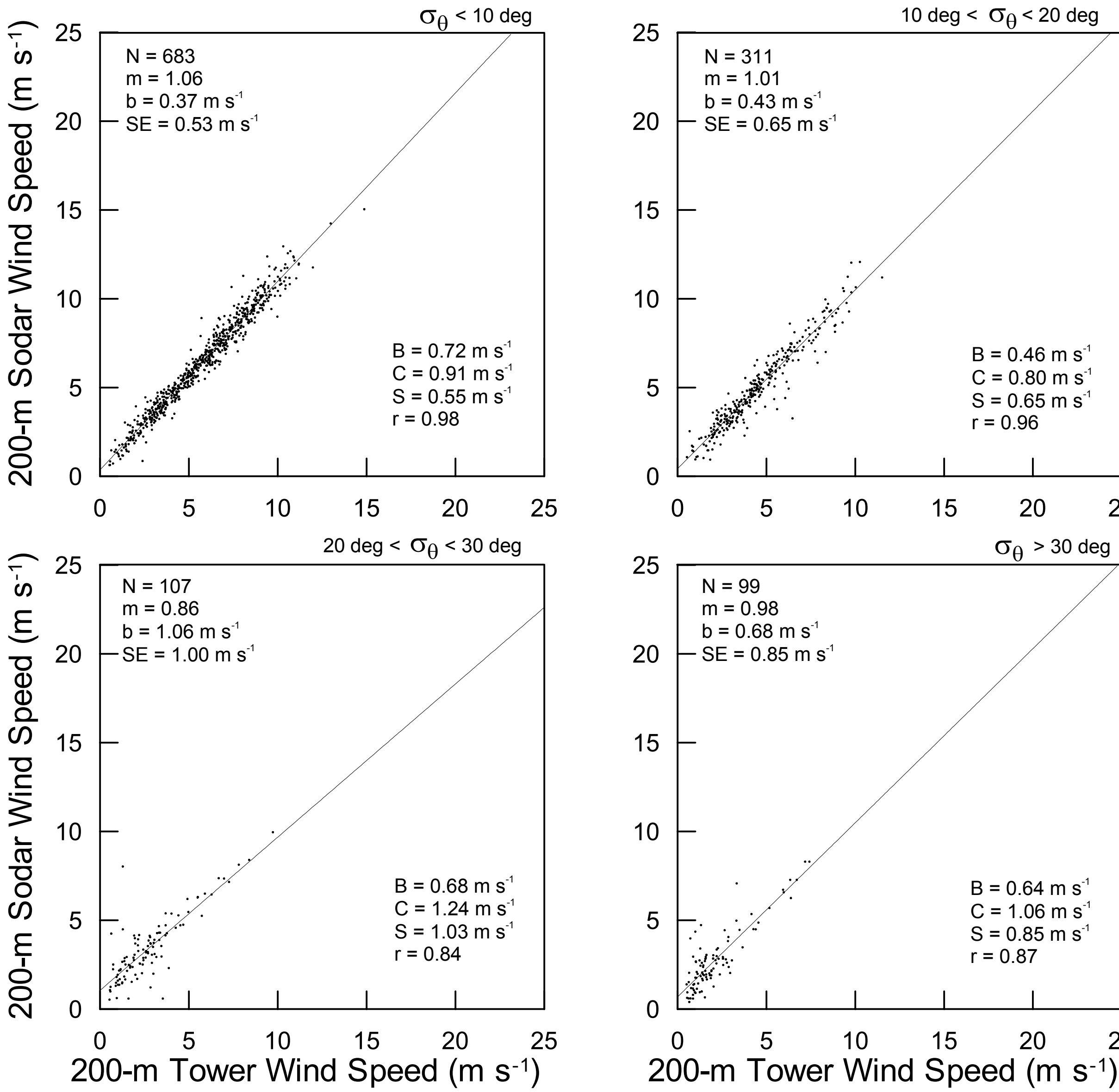

Fig. 1. Example of wind speed scatter plot as a function of σ_θ.

With aggressive QA and QC procedures, sodars are capable of acquiring high quality wind data. However, great care must be taken when interpreting statistical comparisons, especially when those data are acquired during convective and light-wind conditions.

7. REFERENCES

Baxter, R. A., 1995: Performance auditing of sodars under the new USEPA guidance – applications of a new instrument to quantitatively assess sodar performance. *Ninth Sym. on Meteor. Obs. and Instrum.*, Charlotte, NC, Amer. Meteor. Soc., 442-446.

Baxter, R. A., 1996: Quality assurance of remote wind profilers during the 1995 EPA Sodar Characterization Study. *Ninth Joint Conf. on Applications of Air Pollution Meteor. with AWMA*, Atlanta, GA, Amer. Meteor. Soc., 556-560.

Coulter, C. T., 1994: An evaluation of a solar radiation/delta-T method for estimating Pasquill-Gifford (P-G) stability categories. *Eighth Joint Conf. on Applications of Air Pollution Meteor. with AWMA*, Nashville, TN, Amer. Meteor. Soc., 40-47.

Crescenti, G. H., 1997: A look back on two decades of Doppler sodar comparison studies. *Bull. Amer. Meteor. Soc.*, **78**, 651-673.

Crescenti, G. H., 1998: The degradation of Doppler sodar performance due to noise: A review. *Atmos. Environ.*, **32**, 1499-1509.

Crescenti, G. H., 1999: A study to characterize performance statistics of various ground-based remote sensors. NOAA Tech. Memo. ERL ARL-229, Silver Spring, MD, 286 pp.

Crescenti, G. H., and R. A. Baxter, 1998: Examples of noise interference on Doppler sodar performance. *Tenth Sym. on Meteor. Obs. and Instrum.*, Phoenix, AZ, Amer. Meteor. Soc., 228-232.

Crosby, D. S., L. C. Breaker, and W. H. Gemmill, 1993: A proposed definition for vector correlation in geophysics: theory and application. *J. Atmos. Oceanic Technol.*, **10**, 355-367.

Gaynor, J. E., 1979: The importance of moisture fluctuations and wind shear in acoustic backscatter in GATE. *J. Appl. Meteor.*, **18**, 1472-1480.

Hoehne, W. E., 1971: Standardized functional tests. NOAA Tech. Memo. NWST&EL-12, U. S. Department of Commerce, 23 pp.

Kaimal, J. C., 1986: Flux and profile measurements from towers in the boundary layer. *Probing the Atmospheric Boundary Layer*, D. H. Lenschow, Ed., Amer. Meteor. Soc., 19-28.

Stull, R. B., 1988: An *Introduction to Boundary Layer Meteorology*. Kluwer Academic Publishers, Dordrecht, 666 p.

U. S. Environmental Protection Agency, 1987 (revised 1999): On-Site Program Guidance for Regulatory Modeling Applications. EPA-450/4-87-103, Office of Air Quality Planning and Standards, Research Triangle Park, NC.

U. S. Environmental Protection Agency, 1995: Quality Assurance Handbook for Air Pollution Measurement Systems, Volume IV: Meteorological Measurements. EPA-600/R-94/038d, Office of Research and Development, Research Triangle Park, NC.

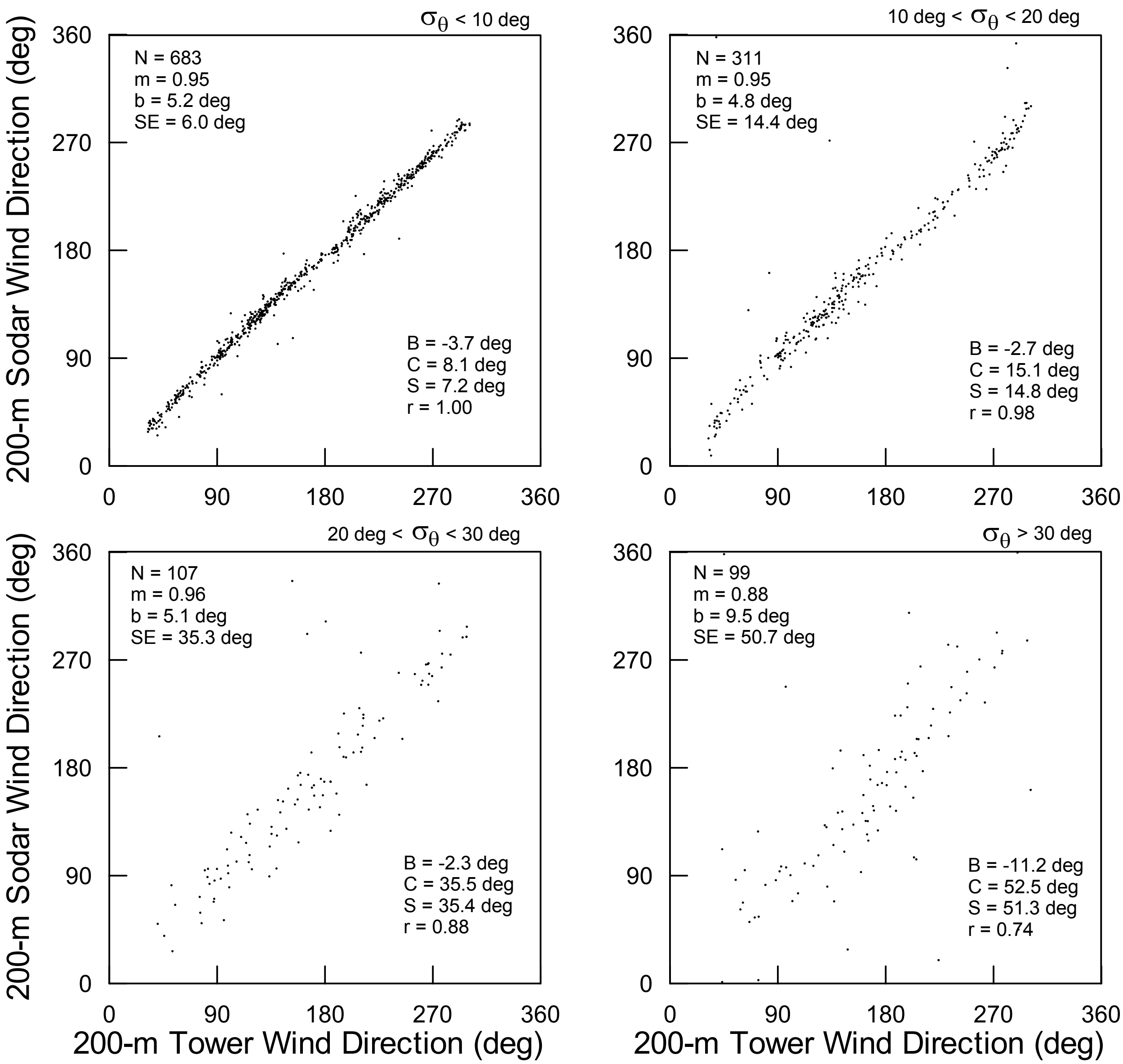

Fig. 2. Example of wind direction scatter plot as a function of σ_θ.